# A NATURE-INSPIRED, DROPLET-SHAPED FLOATING PLATFORM FOR OFFSHORE WIND TURBINES

Mahmud Ismayilov

Azerbaijan State Oil and Industry University, Baku, AZERBAIJAN
ismahmud17630@sabah.edu.az

**Abstract**

*Floating offshore wind energy harnesses high-quality wind resources in deep waters, but traditional platform designs face challenges in mitigating extreme marine forces and maintaining cost-effectiveness. This paper introduces a nature-inspired, droplet-shaped floating platform that addresses these challenges through innovative design and hydrodynamic optimization. Conventional floating platforms such as Spar, Tension Leg Platform (TLP), and Semi-Submersible concepts each provide unique advantages, including stability, reduced motion, and robust mooring systems, yet encounter limitations like extreme load variability and high dynamic response under harsh conditions. Drawing inspiration from the streamlined geometry of water droplets, the proposed platform leverages biomimetic principles to enhance hydrodynamic efficiency, minimize drag, and improve stability. A mathematical framework is developed to define the droplet shape, integrating linear and semicircular functions to optimize angles, radii, and submerged volumes. Analytical derivations establish boundary conditions, enabling precise calculations for structural parameters and buoyancy. The droplet-shaped design aims to mitigate pitch, heave, and surge motions, offering a robust foundation for supporting multi-megawatt wind turbines in extreme environments. This study proposes a cost-effective, scalable alternative to existing platforms, highlighting the potential of biomimicry to revolutionize floating offshore wind technology. Further validation through numerical simulations and experimental wave-tank testing is recommended to optimize performance and reliability. This novel approach signifies a step toward innovative, sustainable solutions for harnessing renewable energy in deep-water regions, paving the way for the next generation of offshore wind deployment.*

**Keywords:** Floating offshore wind, droplet-shaped platform, biomimetic design, hydrodynamic optimization, renewable energy, multi-megawatt turbines

## 1. Introduction

The exploitation of offshore wind resources in deep-water environments represents one of the most promising pathways toward sustainable energy generation. Conventional floating platforms—including Spar, Semi-Submersible, and Tension Leg Platforms (TLP)—offer partial advantages in terms of stability and load management, but they are limited by large dynamic responses, extreme loading conditions, and high construction costs. Addressing these challenges requires innovative geometries that enhance hydrodynamic efficiency while ensuring structural robustness.

This study introduces and develops a biomimetic droplet-shaped floating platform, inspired by naturally optimized hydrodynamic forms observed in water droplets, icebergs, and marine mammals. The central premise is that the droplet's streamlined profile can substantially reduce drag forces, minimize pitch, surge, and heave motions, and optimize buoyancy distribution. A mathematical framework is formulated to define the geometry of the droplet, integrating linear and semicircular functions subject to specific boundary conditions. Analytical derivations provide

closed-form solutions for volume, cross-sectional area, and buoyancy requirements, enabling scalability for multi-megawatt turbine applications.

The proposed design offers a cost-effective and hydrodynamically efficient alternative to traditional platforms. By leveraging biomimetic principles, the droplet-shaped concept aims to mitigate extreme environmental loads, improve structural survivability, and enhance performance under harsh marine conditions. The geometry further demonstrates potential scalability and adaptability, aligning with current industrial needs for robust, deployable solutions in deep-water regions.

Future research will focus on numerical and experimental validation of the proposed concept. High-fidelity Computational Fluid Dynamics (CFD) simulations, coupled aero-hydro-elastic modeling, and wave-basin testing are recommended to assess drag coefficients, hydrodynamic stability, and long-term fatigue behavior. Additional investigations into mooring-line configurations and material optimization will strengthen the platform's applicability for commercial deployment.

In conclusion, this thesis advances floating offshore wind technology by presenting a nature-inspired structural paradigm that unites mathematical precision with biomimetic insight. The droplet-shaped platform contributes to the development of next-generation offshore wind systems by offering enhanced stability, reduced costs, and sustainable scalability, thereby supporting the global transition toward renewable energy.

## 2. Methodology

One of the most aerodynamically and hydrodynamically stable shapes found in nature is the droplet (Figure 1). Its streamlined geometry minimizes resistance and maximizes stability, making it an ideal inspiration for various design applications. This natural form is not only visually elegant but also functionally optimized, as it allows for minimal drag in both air and water. When a droplet falls, it adopts a shape that balances surface tension, gravitational forces, and fluid dynamics, forming an efficient structure that reduces energy loss.

**Figure 1.** A Droplet Hanging from a Leaf, Illustrating Natural Streamlined Geometry

The principles derived from these natural forms have far-reaching applications in engineering and design. For instance, they inspire the hydrodynamic profiles of ships, submarines, and now floating wind turbine platforms. By mimicking the droplet's streamlined structure, these platforms can achieve reduced drag, improved stability, and enhanced durability, even in harsh marine environments. The droplet serves as a testament to nature's ability to create solutions that balance form and function, making it a cornerstone for biomimetic engineering.

As depicted in Figure 2, the shape of an iceberg closely resembles an inverted droplet beneath the water, with its wide base providing stability, while the portion above water mimics the shape of a falling droplet. This dual geometry plays a critical role in its ability to remain resilient against dynamic marine forces. The submerged section, which constitutes the majority of the iceberg's mass, provides buoyancy and resists tipping by maintaining a low center of gravity. Meanwhile, the above-water portion serves as a streamlined form, reducing wind resistance and minimizing wave impacts on the exposed surface. This natural design is an exquisite example of evolutionary optimization for harsh environments. Icebergs are subjected to constant wave motion, varying currents, and environmental changes, yet their shape ensures equilibrium and durability. The droplet-like profile beneath the waterline contributes to smooth hydrodynamic interactions, effectively dissipating energy from waves and stabilizing the iceberg. Additionally, the wide submerged base enhances the structural balance, acting as a natural counterweight to the forces acting above the water. In the context of engineering, the iceberg's structure offers invaluable insights into designing offshore platforms. Its dual nature—a wide, stable base and a streamlined, minimal-resistance profile—can inspire floating structures that must endure similar challenges, such as strong ocean currents, high winds, and rough seas.

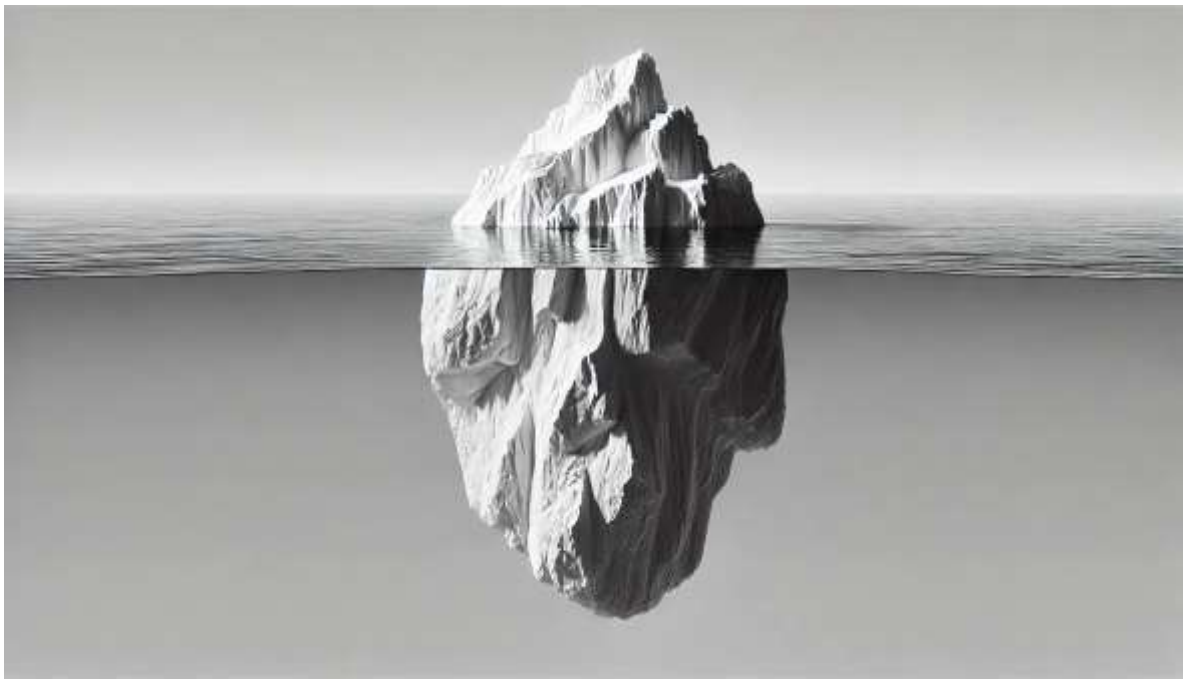

**Figure 2.** An Iceberg with Submerged and Above-Water Portions, Demonstrating Natural Hydrodynamic Stability.

Similarly, large marine mammals such as whales (Physeter macrocephalus) demonstrate remarkable balance and stability. These creatures have been observed resting near the water's surface in a vertical position, relying on their streamlined bodies and slight movements to maintain equilibrium. Studies, such as those published in Current Biology (Miller et al., 2008), reveal that

whales often enter brief, near-vertical resting states. During these periods, they leverage their body shape to stabilize themselves, even amidst surface currents and wave activity [33].

As illustrated in Figure 3, the body of a whale resembles an inverted droplet, further emphasizing the prevalence of this efficient geometry in nature. This alignment between form and function provides critical insights for biomimetic design. By studying these natural examples, we can develop advanced engineering solutions, such as stable and efficient offshore platforms. The droplet-shaped geometry serves as a guiding principle, enabling the creation of structures that not only withstand environmental challenges but also operate efficiently in dynamic marine conditions.

**Figure 3.** Whales Resting in a Vertical Position, Exemplifying Natural Hydrodynamic Balance [34].

Likewise, centuries of trial and error have led to the development of highly effective fishing floats, which serve as simple yet robust markers on the water. Their shapes have evolved to minimize oscillations, maintain buoyancy, and reliably signal fish bites, as shown in Figure 4. Notably, fishing floats share a key objective with floating wind turbine platforms—namely, remaining upright and stable in a dynamic marine environment. Although wind turbines operate at a vastly different scale and carry much heavier loads, the underlying principle of distributing volume and mass for optimal stability is remarkably similar.

**Figure 4.** Various Fishing Floats Showcasing Hydrodynamically Stable Designs.

By integrating such natural design insights, the droplet-shaped floating platform proposed in this study mimics the hydrodynamic advantages of streamlined shapes found in nature. Its tapered submerged profile, akin to an iceberg's hidden volume or a whale's vertical resting posture, aims to minimize drag and wave excitation forces. This approach directly supports the platform's goals of reducing pitch, heave, and surge motions while providing the buoyancy required to support multi-megawatt turbines under extreme conditions.

To translate these principles into a functional design, the study employs a mathematical framework to define the droplet shape with precision. By systematically analyzing the relationships between boundary conditions, geometric parameters, and hydrodynamic performance, the design ensures maximum stability and efficiency.

The mathematical model, depicted in Figure 5, illustrates a mathematical representation of the drop shape, which can be obtained by rotating the function $f_1(x) = x \cdot \tan\alpha$ (1) over the interval $[x_1, x_3]$ and the function $f_2(x) = \sqrt{y_3^2 - (x - x_4)^2}$ (2) over the interval $[x_3, x_5]$ around the x-axis.

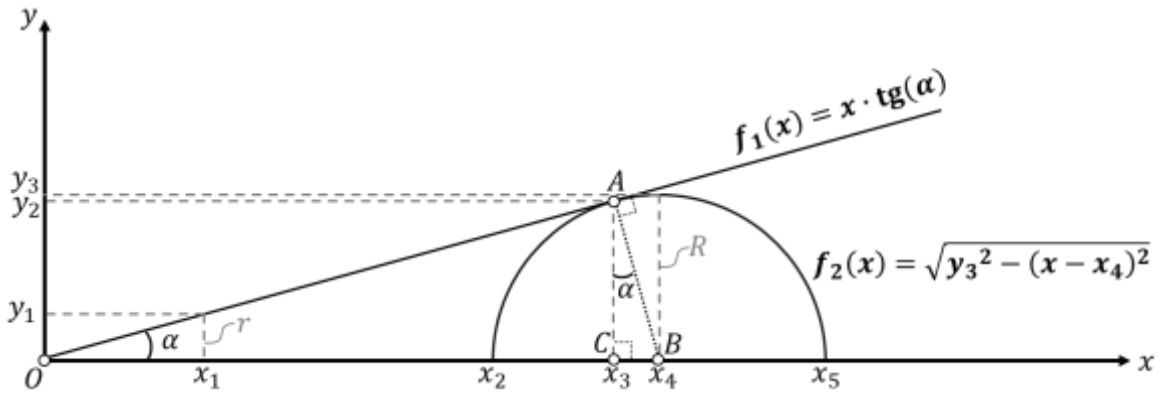


**Figure 5.** Mathematical Model of Drop Shape Defined by Boundary Conditions.

From Figure 5, we aim to determine the values of all relevant coordinates by applying the defined boundary conditions and using the mathematical model of the drop's shape. The boundary conditions are as follows:

1. *First Boundary:*

$$y_1 = r \tag{3}$$

Here, $r$ is the top radius of the conical section in the droplet's profile. This boundary corresponds to the narrower (lower) limit of the droplet shape.

2. *Second Boundary:*

$$y_3 = R \tag{4}$$

Here, $R$ denotes the radius of the semicircle and represents the largest cross-sectional width (upper limit) of the droplet.

3. *Third Boundary:*

$$x_1 = r \cdot \cot\alpha = r \cdot \frac{\cos\alpha}{\sin\alpha} \tag{5}$$

This condition defines the horizontal position of the boundary as a function of the angle of inclination, $\alpha$. Here, $\alpha$ is the angle between the tangent at the boundary and the horizontal axis.

From triangles OAB and ABC in Figure 5 we can see that:

1) AB is the radius of the semicircle which is equal to R:

$$AB = R \tag{6}$$

2) From triangle OAB:

$$\sin\alpha = \frac{AB}{OB} = \frac{R}{x_4} \tag{7}$$

3) From triangle ABC:

$$\cos\alpha = \frac{AC}{AB} = \frac{y_2}{R} \tag{8}$$

From (7) we will find $x_4$:

$$x_4 = \frac{R}{\sin\alpha} \tag{9}$$

From (8) we will find $y_2$:

$$y_2 = R \cdot \cos\alpha \tag{10}$$

From (1) and (10) we will find $x_3$:

$$f_1(x_3) = y_2 = R \cdot \cos\alpha = x_3 \cdot \tan\alpha$$

then

$$x_3 = R \cdot \frac{\cos\alpha}{\tan\alpha} = R \cdot \cot\alpha \cdot \cos\alpha = R \cdot \frac{\cos^2\alpha}{\sin\alpha} \tag{11}$$

From Figure 5 we can see that:

$$x_2 = x_4 - R \tag{12}$$

and

$$x_5 = x_4 + R \tag{13}$$

From (9) and (12) we find $x_2$:

$$x_2 = \frac{R}{\sin\alpha} - R = R \cdot \left(\frac{1}{\sin\alpha} - 1\right) \tag{14}$$

From (9) and (13) we find $x_5$:

$$x_5 = \frac{R}{\sin\alpha} + R = R \cdot \left(\frac{1}{\sin\alpha} + 1\right) \tag{15}$$

After defining analytical values all vertical $y_1, y_2, y_3$ and horizontal $x_1, x_2, x_3, x_4, x_5$ coordinates we will write them into Table 1.

**Table 1.** Analytical Values of Vertical and Horizontal Coordinates for the Drop Shape with given boundary conditions r, R and $\alpha$.

| **Vertical Coordinates (y):** | **Horizontal Coordinates (x):** |
|---|---|
| $f_1(x) = x \cdot \tan\alpha$ | $x_1 = r \cdot \frac{\cos\alpha}{\sin\alpha}$ |
| $f_2(x) = \sqrt{R^2 - \left(x - \frac{R}{\sin\alpha}\right)^2}$ | $x_2 = R \cdot \left(\frac{1}{\sin\alpha} - 1\right)$ |
| $y_1 = r$ | $x_3 = R \cdot \frac{\cos^2\alpha}{\sin\alpha}$ |
| $y_2 = R \cdot \cos\alpha$ | $x_4 = \frac{R}{\sin\alpha}$ |
| $y_3 = R$ | $x_5 = R \cdot \left(\frac{1}{\sin\alpha} + 1\right)$ |

Table 1 represents all coordinates values for defining drop shape that represented by combination of two functions: linear function $f_1(x) = x \cdot \tan\alpha$ and semicircular function $f_2(x) = \sqrt{y_3^2 - (x_3 - x_4)^2}$ with offset $x_4$.

The total volume for drop shape represented by combination of two functions: linear function - $f_1(x) = x \cdot \tan\alpha$ and semicircular function - $f_2(x) = \sqrt{y_3^2 - (x - x_4)^2}$ with offset $x_4$ will be calculated as:

1. For the interval $[x_1, x_3]$:

$$V_1 = \pi \int_{x_1}^{x_3} [f_1(x)]^2 \, dx$$

2. For the interval $[x_3, x_5]$:

$$V_2 = \pi \int_{x_3}^{x_5} [f_2(x)]^2 \, dx$$

The total volume of the drop is given by:

$$V_{total} = V_1 + V_2 = \pi \int_{x_1}^{x_3} [f_1(x)]^2 \, dx + \pi \int_{x_3}^{x_5} [f_2(x)]^2 \, dx \tag{16}$$

Substituting the limits in (16) from Table 1, the total volume is:

$$V_{total} = \pi \cdot \left\{ \int_{r \cdot \frac{\cos\alpha}{\sin\alpha}}^{R \cdot \frac{\cos^2\alpha}{\sin\alpha}} (x \cdot \tan\alpha)^2 \, dx + \int_{R \cdot \frac{\cos^2\alpha}{\sin\alpha}}^{R \cdot \left(\frac{1}{\sin\alpha}+1\right)} \left[ \sqrt{R^2 - \left(x - \frac{R}{\sin\alpha}\right)^2} \right]^2 dx \right\} \tag{17}$$

After solving and simplifying (17):

$$V_{drop} = \frac{\pi \cdot [(1 + \sin\alpha)^2 \cdot R^3 - r^3 \cdot \cos\alpha]}{3 \cdot \sin\alpha} \tag{18}$$

When designing a floating body, the buoyant force—determined by the weight of the displaced (submerged) water—must equal the total weight of the structure itself, including both the platform and the wind turbine. Because we can calculate the required displaced-water volume, it is crucial to express all geometric relationships in terms of that submerged volume. In our case, these geometric unknowns are r (the smaller radius of the droplet), R (the maximum radius of the droplet), and the angle $\alpha$. Rearranging the volume formula (18) for R gives:

$$R(V_{drop}) = \sqrt[3]{\frac{3 \cdot V \cdot \sin\alpha + \pi \cdot r^3 \cdot \cos\alpha}{\pi \cdot (1 + \sin\alpha)^2}} \tag{19}$$

In this study, $r$ is assumed to be equal to the wind turbine tower's bottom diameter. Meanwhile, $\alpha$ can be obtained experimentally or via simulations of drag force, since the angle affects the frontal cross section on which the drag force depends.

The cross-sectional area A of the droplet-shaped platform can be found by integrating the functions $f_1(x)$ and $f_2(x)$ (without rotation), namely:

$$A = 2 \cdot \int_{x_1}^{x_3} f_1(x)dx + \int_{x_3}^{x_5} f_2(x)dx \tag{20}$$

After evaluating these integrals, the result is:

$$A = (R^2 - r^2) \cdot \cot\alpha + R^2 \cdot \left(\frac{\pi}{2} + \alpha\right) \tag{21}$$

where

$$\alpha \in \left[0; \frac{\pi}{2}\right]$$

When analyzing the hydrodynamic performance of the droplet-shaped platform, it is important to consider the drag force, $F_{drag}$. This force is given by:

$$F_{drag} = \frac{1}{2}\rho v^2 \cdot A \cdot C_D$$

where ϱ is the fluid (or air) density, $v$ is the flow velocity, $A$ is the characteristic area (often taken as the projected area on the plane perpendicular to the velocity vector), and $C_D$ is the drag coefficient, determined experimentally or via CFD simulations.

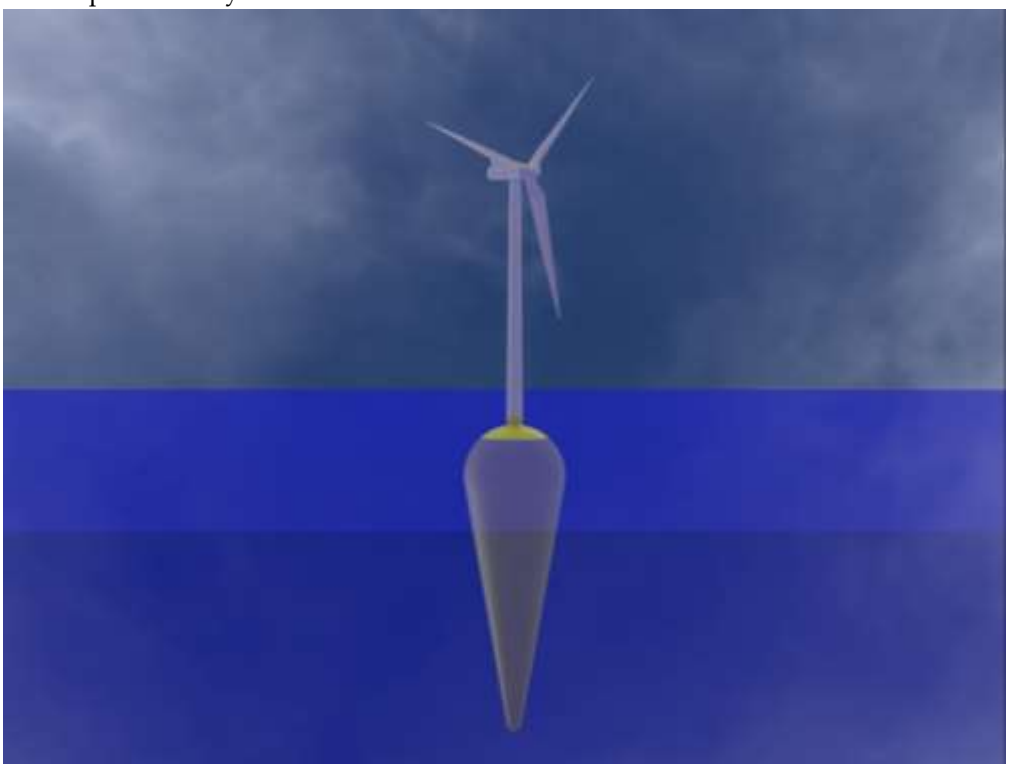

**Figure 6.** Design concept of droplet-shaped floating platform for offshore wind turbines.

Understanding and accurately estimating $F_{\text{drag}}$ is essential for evaluating the platform's overall stability and performance, particularly under high wind and wave conditions.

The mathematical derivations described thus far form the foundation for a biomimetic droplet-shaped platform, which aims to balance hydrodynamic efficiency with sufficient buoyancy for multi-megawatt wind turbines. By systematically arranging the conical lower section and semicircular upper region, the design seeks to reduce wave-induced motions and structural loads. To offer a

clearer perspective, Figure 6 presents a conceptual rendering of the droplet-shaped floating platform, highlighting its overall geometry, approximate immersion depth, and turbine placement.

As illustrated in Figure 6, the narrow base of the platform transitions into a broader hull near the water surface, maximizing stability and minimizing wave-excitation forces. The conical profile in the submerged section helps control hydrodynamic drag and vertical motions, whereas the semicircular upper portion enhances buoyancy and overall structural robustness. This integrated form directly corresponds to the derived volume expressions and boundary conditions outlined earlier, ensuring that the required displaced water volume can support the turbine's mass while maintaining optimal trim and pitch characteristics. It is recommended to conduct numerical simulations and wave-tank tests to refine the droplet-inspired geometry and validate its performance under various operational and extreme sea conditions.

## 3. Conclusion

1. This paper introduced a biomimetic droplet-shaped floating platform designed to harness wind energy in deep-water regions. The proposed geometry combines a linear (conical) function with a semicircular profile to mitigate extreme wave-induced loads and platform motions—specifically pitch, heave, and surge—while supporting multi-megawatt wind turbines.
2. Analytical formulations were provided for boundary conditions, key geometric parameters, total volume, cross-sectional area, and drag force. These closed-form expressions facilitate rapid estimation of buoyancy requirements based on a targeted submerged volume, simplifying scaling for different turbine capacities.
3. The droplet-shaped platform concept leverages efficient hydrodynamic principles inspired by nature, offering the potential for improved motion response in harsh marine environments.
4. Validation of this geometry through numerical simulations, including coupled aero-hydro-elastic analyses, and wave-basin experiments is recommended to confirm its performance and reliability.
5. Further studies should focus on exploring mooring-line layouts, structural optimization, and cost trade-offs. These aspects are critical for refining the platform design and enhancing its practical implementation.
6. This innovative approach aims to advance floating offshore wind technology by providing a hydrodynamically efficient and adaptable solution suited to a wide range of environmental conditions.

**CONFLICT OF INTEREST**

Authors declare that they do not have any conflict of interest

## References

1. Konispoliatis, D. N., Katsaounis, G. M., Manolas, D. I., Soukissian, T. H., Polyzos, S., Mazarakos, T. P., Voutsinas, S. G., & Mavrakos, S. A. (2021). REFOS: A renewable energy multi-purpose floating offshore system. Energies, 14(11), 3126. https://doi.org/10.3390/en14113126

2. Wang, S., & Moan, T. (2024). Analysis of extreme internal load effects in columns in a semi-submersible support structure for large floating wind turbines. Ocean Engineering, 291, 116372. https://doi.org/10.1016/j.oceaneng.2023.116372

3. Mohseni, M., & Guedes Soares, C. (2024). CFD analysis of wave loading on a 10 MW TLP-type offshore floating wind turbine in regular waves. Ocean Engineering, 301, 117540. https://doi.org/10.1016/j.oceaneng.2024.117540

4. El Beshbichi, O., Xing, Y., & Ong, M. C. (2022). Comparative dynamic analysis of two-rotor wind turbine on spar-type, semi-submersible, and tension leg floating platforms. Ocean Engineering, 266, 112926. https://doi.org/10.1016/j.oceaneng.2022.112926

5. Zhang, W., Calderon-Sanchez, J., Duque, D., & Souto-Iglesias, A. (2024). Computational Fluid Dynamics (CFD) applications in Floating Offshore Wind Turbine (FOWT) dynamics: A review. Applied Ocean Research, 150, 104075. https://doi.org/10.1016/j.apor.2024.104075

6. Yang, Q., Li, D., Xiao, T., Chang, H., Fu, X., & Wang, H. (2024). Control mechanisms of different bionic structures for hydrofoil cavitation. Ultrasonics Sonochemistry, 102, 106745. https://doi.org/10.1016/j.ultsonch.2023.106745

7. Souza, C. E. S., & Bachynski-Polić, E. E. (2022). Design, structural modeling, control, and performance of 20 MW spar floating wind turbines. Marine Structures, 84, 103182. https://doi.org/10.1016/j.marstruc.2022.103182

8. Li, H., Gao, Z., Bachynski-Polić, E. E., Zhao, Y., & Fiskvik, S. (2023). Effect of floater flexibility on global dynamic responses of a 15-MW semi-submersible floating wind turbine. Ocean Engineering, 286, 115584. https://doi.org/10.1016/j.oceaneng.2023.115584

9. Rongé, É., Peyrard, C., Venugopal, V., Xiao, Q., Johanning, L., & Benoit, M. (2023). Evaluation of second and third-order numerical wave-loading models for floating wind TLPs. Ocean Engineering, 288, 116064. https://doi.org/10.1016/j.oceaneng.2023.116064

10. Lopez-Olocco, T., Liang, G., Medina-Manuel, A., Saavedra Ynocente, L., Jiang, Z., & Souto-Iglesias, A. (2023). Experimental comparison of a dual-spar floating wind farm with shared mooring against a single floating wind turbine under wave conditions. Engineering Structures, 292, 116475. https://doi.org/10.1016/j.engstruct.2023.116475

11. Somoano, M., Trubat, P., Guanche, R., & Molins, C. (2024). Experimental modelling of a novel concrete-based 15-MW spar wind turbine. Ocean Engineering, 309, 118612. https://doi.org/10.1016/j.oceaneng.2024.118612

12. Bernal-Camacho, D. F., Mendoza, E., Fontes, J. V. H., Echeverria, C., & Vakis, A. I. (2024). Experiments in an enclosed Wave–Wind Flume environment to study the dynamics of a small-scale Floating Offshore Wind Turbine. Journal of Ocean Engineering and Marine Energy, 10 (6), 917–939. https://doi.org/10.1007/s40722-024-00360-y

13. Li, W., Wang, S., Moan, T., Gao, Z., & Gao, S. (2024). Global design methodology for semi-submersible hulls of floating wind turbines. Renewable Energy, 225, 120291. https://doi.org/10.1016/j.renene.2024.120291

14. Xu, Y., Shi, W., Song, Y., & Hou, H. (2024). Hydrodynamics of a Remora-inspired autonomous underwater vehicle approaching and docking to a benchmark submarine. Ocean Engineering, 291, 116447. https://doi.org/10.1016/j.oceaneng.2023.116447

15. Ran, X., Leroy, V., & Bachynski-Polić, E. E. (2023). Hydroelastic response of a flexible spar floating wind turbine: Numerical modelling and validation. Ocean Engineering, 286, 115635. https://doi.org/10.1016/j.oceaneng.2023.115635

16. Jiang, Z., Yang, L., Gao, Z., & Moan, T. (2022). Integrated dynamic analysis of a spar floating wind turbine with a hydraulic drivetrain. Renewable Energy, 201, 608–623. https://doi.org/10.1016/j.renene.2022.10.104

17. Nederkoorn, T. P., & Seyffert, H. C. (2022). Long-term rogue wave occurrence probability from historical wave data on a spatial scale relevant for spar-type floating wind turbines. Ocean Engineering, 251, 110955. https://doi.org/10.1016/j.oceaneng.2022.110955

18. Wang, S., Moan, T., & Gao, Z. (2023). Methodology for global structural load effect analysis of the semi-submersible hull of floating wind turbines under still water, wind, and wave loads. Marine Structures, 91, 103463. https://doi.org/10.1016/j.marstruc.2023.103463

19. Pegalajar-Jurado, A., Bredmose, H., & Borg, M. (2016). Multi-level hydrodynamic modelling of a scaled 10MW TLP wind turbine. Energy Procedia, 94, 124–132. https://doi.org/10.1016/j.egypro.2016.09.206

20. Liu, Q., Bashir, M., Huang, H., Miao, W., Xu, Z., Yue, M., & Li, C. (2025). Nature-inspired innovative platform designs for optimized performance of floating vertical axis wind turbines. Applied Energy, 380, 125120. https://doi.org/10.1016/j.apenergy.2024.125120

21. Lauria, A., Loprieno, P., Rizzo, F., Severini, A., Foti, D., Leone, E., Francone, A., & Tomasicchio, G. R. (2024). On the effects of wind and operating conditions on mooring line tensions for floating offshore wind turbines. Applied Ocean Research, 152, 104197. https://doi.org/10.1016/j.apor.2024.104197

22. Cousin, A., Delépine, N., Guiton, M., Munoz Zuniga, M., & Perdrizet, T. (2024). Optimal design of experiments for computing the fatigue life of an offshore wind turbine based on stepwise uncertainty reduction. Structural Safety, 110, 102483. https://doi.org/10.1016/j.strusafe.2024.102483

23. Natarajan, S. G., & Rose, B. R. J. (2022). Performance enhancement of futuristic airplanes by nature-inspired biomimetic fish scale arrays: A design approach. Biomimetic Intelligence and Robotics, 2, 100045. https://doi.org/10.1016/j.birob.2022.100045

24. Farr, H., Ruttenberg, B., Walter, R. K., Wang, Y.-H., & White, C. (2021). Potential environmental effects of deepwater floating offshore wind energy facilities. Ocean and Coastal Management, 207, 105611. https://doi.org/10.1016/j.ocecoaman.2021.105611

25. Payenda, M. A., Wang, S., Jiang, Z., & Prinz, A. (2024). Prediction of mooring dynamics for a semi-submersible floating wind turbine with recurrent neural network models. Ocean Engineering, 313, 119490. https://doi.org/10.1016/j.oceaneng.2024.119490

26. Leimeister, M., & Kolios, A. (2021). Reliability-based design optimization of a spar-type floating offshore wind turbine support structure. Reliability Engineering and System Safety, 213, 107666. https://doi.org/10.1016/j.ress.2021.107666

27. Tian, H., Soltani, M. N., & Nielsen, M. E. (2023). Review of floating wind turbine damping technology. Ocean Engineering, 278, 114365. https://doi.org/10.1016/j.oceaneng.2023.114365

28. Firdaus, N., Ali, B., Adiputra, R., Prabowo, A. R., Puryantini, N., & Huda, N. (2023). The dynamic parameters of a spar-type floating offshore wind turbine: A benchmarking assessment. Procedia Structural Integrity, 48, 58–64. https://doi.org/10.1016/j.prostr.2023.07.110

29. Edwards, E. C., Holcombe, A., Brown, S., Ransley, E., Hann, M., & Greaves, D. (2024). Trends in floating offshore wind platforms: A review of early-stage devices. Renewable and Sustainable Energy Reviews, 193, Article 114271. https://doi.org/10.1016/j.rser.2023.114271

30. Gao, C., Liu, Z., Shen, T., Cheng, Z., Chen, F., Liu, S., Jiang, L., & Dong, Z. (2024). Water lily-inspired notch for passive stabilization in floating devices. Device, 2(100405). https://doi.org/10.1016/j.device.2024.100405

31. Machado, M. R., & Dutkiewicz, M. (2024). Wind turbine vibration management: An integrated analysis of existing solutions, products, and open-source developments. Energy Reports, 11, 3756–3791. https://doi.org/10.1016/j.egyr.2024.03.014

32. Jin, B., Lu, Y., Zhang, X., Zhang, X., Li, D., Liu, Q., Deng, B., & Li, H. (2023). Iceberg-inspired solar water generator for enhanced thermoelectricity–freshwater synergistic production. Chemical Engineering Journal, 143906. https://doi.org/10.1016/j.cej.2023.143906

33. Miller, P. J. O., Aoki, K., Rendell, L. E., & Amano, M. (2008). Stereotypical resting behavior of the sperm whale. Current Biology, 18(1), R21–R23. https://doi.org/10.1016/j.cub.2007.11.003

34. National Geographic. (n.d.). Sperm whales nap in vertical positions: A rare look at their resting behavior. Retrieved January 22, 2025, from https://www.nationalgeographic.com/photography/article/sperm-whales-nap-sleeping-photography-spd